Constitutively active mutants of 5-HT 4 receptors are they in unique active states?

Sylvie Claeysen, Michèle Sebben, Carine Becamel, Marie-Laure Parmentier, Aline Dumuis, Joël Bockaert

Constitutively active mutants of 5-HT$_4$ receptors are they in unique active states?

Sylvie Claeysen, Michèle Sebben, Carine Bécamel, Marie-Laure Parmentier, Aline Dumuis, and Joël Bockaert*

UPR CNRS 9023, 141 rue de la Cardonille, 34094 Montpellier Cedex 5, France
*Corresponding Author. Tel: +33 4 67 14 29 30; Fax: +33 4 67 54 24 32;
E-mail: upr9023@ccipe.montp.inserm.fr

Abstract

Somatic mutations leading to constitutively active G-protein coupled receptors (GPCRs) are responsible for certain human diseases. A consistent structural description of the molecular change underlying the conversion of GPCRs from an inactive R state to an active R* state is lacking. Here, we show that a series of constitutively active 5-HT$_4$ receptors (mutated or truncated in the C-terminal and the third intracellular loop) were characterized by an increase in their denaturation rate at 55°C. The thermal denaturation kinetics were monophasic, suggesting that we were measuring mainly the denaturation rate of R*. Analysis of these kinetics revealed that constitutively active C-terminal domain mutants, were due to a change in the *J* constant governing the R/R* equilibrium. However, the constitutive activity of the receptor mutated within the third intracellular loop was the result of both a change in the allosteric *J* constant and a change in the R* conformation.

INTRODUCTION

Recent models describing activation of G-protein coupled receptors (GPCRs) propose the existence of an equilibrium between two functionally distinct states of [R]: the inactive R and the active R* states governed by the allosteric constant J = [R]/[R*]. This two-state allosteric model was introduced by Monod *et al.* (1965) and applied to GPCRs by Samama *et al.* (1993) and Leff (1995). In the absence of agonists, the equilibrium between R and R* determines the level of basal receptor activity. The efficacy of a ligand is thought to be a function of its relative affinity for R and R*. Neutral antagonists have equal affinity for both states, agonists have a higher affinity for R*, whereas inverse agonists have a higher affinity for R (Kjelsberg *et al.*, 1992; Samama *et al.*, 1993; Kenakin, 1996). In the absence of agonists, it can therefore be expected that the percentage of GPCRs in the R* state is low due to important conformational constraints that are released upon activation (Scheer *et al.*, 1996; Gether *et al.*, 1997; Gether and Kobilka, 1998). Previously, we have experimentally determined the J constant for wild type (WT) 5-HT_4 receptors (5-HT_4Rs) expressed in COS-7 cells, and found it to be equal to 6.15, thus indicating that 14% of receptors were in the R* state in the absence of ligands (Claeysen *et al.*, 2000). However, a large series of mutated GPCRs have been found to have a high constitutive activity in the absence of agonists. When naturally occurring, these mutations initiate human diseases such as retinitis pigmentosa, toxic hyperthyroid adenomas, precocious puberty and neonatal severe hypercalcaemia (Van Sande *et al.*, 1995; Spiegel, 1996). In this context, the molecular changes underlying the conversion of R to R* are of particular importance, which despite the progress made in this direction using the information provided by the functional analysis of mutated receptors and from molecular dynamic analysis (Scheer *et al.*, 1996; Bockaert and Pin, 1999) are still poorly understood. One fundamental question is to know whether activating mutations results from an alteration of the J constant, as generally thought (Tiberi and Caron, 1994; Scheer *et al.*, 1996), or if different R* conformations are generated. We have shown recently that two constitutively active 5-HT_4Rs, an i_3 loop mutant (A258L) and a C-terminal truncated mutant (Δ327), are characterized by a modification of the J constant (Claeysen *et al.*, 2000). The J constant modification led to an increase of the relative concentration of R* from 14% in WT to 56% in the mutants (Claeysen *et al.*, 2000).

The aim of this study was to compare and analyse the thermal denaturation kinetics of a series of constitutively active mutated 5-HT_4Rs, and to determine whether they can be described by a simple change in the J constant, or if they reveal an additional change in the R* conformation.

RESULTS AND DISCUSSION

We first compared the structural stability of WT 5-HT_4Rs to that of two mutated 5-HT_4Rs, the truncated C-terminal 5-HT_4R (Δ327) and the i3 (third intracellular loop) 5-HT_4R (A258L) mutant (Claeysen *et al.*, 2000). All three receptors were expressed at similar expression density in COS-7 cells (2000–3000 fmol/mg). The mutated 5-HT_4Rs had a high constitutive activity, as previously described (Claeysen *et al.*, 2000) and illustrated in Figure 1A.

The WT receptor was particularly stable, such that after a 3 h incubation period at 45°C, no significant denaturation was observed (Figure 1B). However, over the same time period, a 50% denaturation was obtained with the mutated receptors, indicating that the constitutive activation of the 5-HT_4Rs was associated with thermal instability, as previously shown for β_2-adrenergic receptors and histamine H2 receptors (Gether *et al.*, 1997; Alewijnse *et al.*, 2000). Experiments were then performed to compare the t1/2 of denaturation of WT and mutated receptors at 55°C. A 3 h incubation period led to 75% of denaturation of WT and an almost complete denaturation of the mutated receptors (Figure 1B and C).

Western blot analysis of WT and truncated 5-HT_4R (Δ327) indicated that denaturation at 55°C was not associated with a significant proteolysis of receptor proteins (Figure 1E). We also verified that WT, 5-HT_4 (Δ327) and 5-HT_4 (A258L) receptors were similarly targeted to the plasma membranes, as indicated by immunofluorescence observations and [3H]GR 113808 binding measured in intact cells at 4°C (see Figure 2A and B). Note that the ratio between the number of [^{3}H]GR 113808 binding sites determined in intact cells and in particulate fractions was identical, regardless of the nature of the receptor expressed, WT or mutated (Figure 2). Although we may have expected a higher proportion of mutated receptors in intracellular domains, either due to desensitization and internalization of constitutively active receptors or to misfolding, this was not the case in the present study.

The denaturation kinetics of WT, 5-HT4 (Δ327) and 5-HT4 (A258L) mutant receptors were clearly different (Figure (Figure1C).1C). As expected, the denaturation rates were also independent of receptor density, such that no significant differences were observed when denaturation was carried out on membranes prepared from COS-7 cells expressing low or high levels of receptors (data not shown).

A semi-logarithmic transformation of the time-courses (Log[Rt]/[Rt_0] as the function of t with [Rt]= [R] + [R*] and [Rt_0] = [R_0] + [R*$_0$] being the total R concentration [^{3}H]GR 113808 labeled

receptors at *t* and *t* = 0 respectively, allowed the calculation of the $t_{1/2}$ of denaturation. For the WT, 5-HT_4 (Δ327) and 5-HT_4 (A258L) mutant receptors they were equal to 70 ± 4 (n = 10), 17 ± 4 (n = 6) and 48 ± 5 (n = 6) min, respectively (Figure 1D).

We then measured the $t_{1/2}$ of denaturation of other constitutively active mutants (Figure 3). Some were truncated within the end of C-terminal tail (Δ358, Δ346) but have kept the two putatively palmitoylated cysteines (C328, C329), which are likely to anchor 5-HT_4 receptors to the membrane, as shown for many GPCRs. These cysteines are certainly of crucial structural importance since, in addition to being palmitoylated, they have been found to be at the C-terminus of an additional helix (helix VIII) in the crystal structure of rhodopsin (Palczewski *et al.*, 2000). In two others constitutively active mutants, one (C329S) or two (C328–329S) of these cysteines have been substituted with a serine (Figure 3A and B). In many GPCRs, including the β_2-adrenergic receptors, mutation of palmitoylated cysteines leads to constitutively active receptors (Moffett *et al.*, 1996).

The classification of these mutants in order of increasing levels of constitutive activity, were as follows: WT = Δ358 < C329S < Δ346 < C328–329S < Δ327 < A258L (Figure 3B). The corresponding $t_{1/2}$ of denaturation determined as described in Figure 1 were equal to 70 ± 4 (*n* = 10), 68 ± 5 (*n* = 4), 50 ± 4 (*n* = 5), 35 ± 3 (*n* = 4), 23 ± 3 (*n* = 5), 17 ± 4 (*n* = 6), 48 ± 5 (*n* = 6) (Figure 3C).

We propose the following model, where the denaturation of R and R* is governed by the schema:

$$Rd \overset{k_2}{\leftarrow} R \underset{J}{\leftrightarrow} R^* \overset{k_1}{\rightarrow} R^*d$$

, in which Rd and R*d are the denaturated receptors. By measuring the total [^{3}H]GR 113808 binding, we are following the evolution of [R*t*] = [R] + [R*].

The evolution of [R] + [R*] = [R*t*] is described by:

$$\frac{-d([R]+[R^*])}{dt} = \frac{d([Rd]+[R^*d])}{dt} = k_1[R^*] + k_2[R] \qquad \text{(equation 1)}$$

Assuming that the equilibrium between R and R* still exists during *dt*, i.e. we have $J = [R]/[R^*]$, the integration of equation 1 between *t* and $t = 0$ gives:

$$Log\frac{([R]) + [R^*])}{([R_0] + [R^*_0])} = Log\frac{[Rt]}{[Rt_0]} = -\frac{k_1 + k_2 J}{1 + J}t \qquad \text{(equation 2)}$$

Our model predicts that the observed $t_{1/2}$ of denaturation depends on the denaturation constants of the receptors (k_1, k_2) and on the values of *J*.

The denaturation kinetics displayed only one slope, indicating that the denaturation of only one protein conformation was followed (Figures 1D and 3C). One could argue that we followed the denaturation of R* rather than that of R since R* is the more unstable structure. It is likely that, following denaturation of R*, the R→R* equilibrium was shifted to the R* form at a much faster rate than the denaturation rate of R*. Therefore, under our experimental conditions, the observed denaturation kinetic was mainly governed by the denaturation rate of R*. Thus, equation 2 becomes:

$$Log\frac{[Rt]}{[Rt_0]} = -\frac{k_1}{1 + J}t \qquad \text{(equation 3)}$$

and

$$t_{1/2} = \frac{Log(2)}{k_1}(1 + J) \qquad \text{(equation 4).}$$

We had previously determined the *J* constant for the WT and two constitutively active mutants [5-HT_4R (Δ327) and 5-HT_4R (A258L)] Claeysen *et al.*, 2000). Similar experiments allowed us to determine in this study the *J* constants for the other mutants described (see Figure 3 legend).

Therefore, we plotted $t_{1/2}$ against $(1 + J)$ for the WT receptor and the different constitutively active mutants (Figure 3D).

We could see that all the points, except the i3 mutant (A258L), could be fitted by a linear regression (Figure 3D). Indeed, for these points, the regression $t_{1/2} = a\ (1 + J)$ was positive and significant (a = 9.7 ± SE 0.46, p <0.0001). Moreover, neither the inclusion of an non-zero intercept ($t_{1/2} = a\ (1 + J) + b$) nor the inclusion of a quadratic term ($t_{1/2} = a\ (1 + J)^2 + b(1 + J) + c$) significantly improved the fit of the regression (F1,5 = 0.66, *NS* and F1,4 = 0.41, *NS*).

Therefore, for the set of WT and C-tail mutants, $t_{1/2}$ was proportional to $(1 + J)$ as predicted by the model. The denaturation constant k_1 of these receptors can be estimated as 0.071 min^{-1} (with equation 4). However, the i3 mutant (A258L) had clearly a different denaturation rate. Indeed, for a same level of constitutive activity $(1 + J)$ as compared to the mutant Δ327, its k_1 was very different and equal to 0.026 min^{-1} assuming that equation 4 is true for this mutant as it was for the other mutants.

In conclusion, these data show that the WT receptor and the C-tail mutant receptors share the same denaturation constant, whereas the i3 mutant has a clearly different denaturation constant. This indicates that constitutively active mutations can result either from a change in J without any change in the R* conformation or from both a change in J and a change in the R* conformation.

In addition, these results constitute a strong indication that the increase in thermal instability of these mutant receptors was not due to point mutations or truncations per se, but instead, to the intensity of structural changes associated with the release of structural constraints.

To further support this conclusion, we hypothesized that, if the R* form of the receptor is more unstable, due to a release in constraints, the mutations stabilizing the receptor in the R form, could be expected to produce mutant receptors that are more stable than the WT. In family A GPCRs, a conserved Asp residue in TMDII has been shown to be crucial for signal transduction, agonist affinity, allosteric regulation by Na^+, pH and guanyl nucleotides. Substituting this Asp in TMDII for Asn or Ala in the WT receptor (in various family A GPCRs), leads to a silent receptor, unable to trigger the R to R* conformational change (Wang *et al.*, 1991; Sealfon *et al.*, 1995; Fanelli *et al.*, 1999). This observation is consistent with a stabilization of the receptor in the R form. Indeed, introducing this mutation (D66N) in the 5-HT_4R led to a particularly silent receptor with no constitutive activity, regardless of receptor density (Figure 4A). Compared with the WT, this D66N mutated receptor had a similar affinity for the antagonist [^{3}H]GR113808 and for the agonist 5-HT (not shown), and was insensitive to 5-HT (not shown). This indicates that this mutation increases the structural constraints of receptors, thus reducing their spontaneous transition to R*. We were expecting that such an augmentation of the structural constraints of the D66N mutant should increase its $t_{1/2}$ of denaturation (decrease its denaturation rate). This was indeed the case ($t_{1/2}$ = 102 ± 9, n = 5, Figure 4B).

This is the first experimental evidence to show that a mutation which hinders GPCRs from undergoing the R→R* transition, increases their structural stability.

The 'two-state' formalism has been recently recognized to be a simplification of a more general concept of allosteric equilibrium. According to this concept, the receptor undergoes transitions from a large population of allosteric states (Kenakin, 1997; Onaran and Costa, 1997) with different agonists able to stabilize varying populations of active states. Similarly, we can propose that different mutations will stabilize different active states as previously proposed by Parma *et al.* on different experimental basis (Parma *et al.*, 1995). We had previously speculated on the existence of structurally, and therefore pharmacologically different active R* on the following basis: PACAP receptors expressed in LLCPK1 cells can be stimulated by PACAP-38 and PACAP-27, whereas PACAP-27 is consistently more potent in stimulating cAMP formation, compared to PACAP-38, with the latter being more potent in stimulating inositol phosphate accumulation (Spengler *et al.*, 1993). This is indirect evidence demonstrating that different R* entities can exist having different G protein coupling specificity. This, and other similar observations have led to the notion of agonist stimulus trafficking, whereby different agonists, by stabilizing different R* conformations, steer those receptors toward different G protein pathways (Kenakin, 1995; Gudermann *et al.*, 1996).

The present data constitute direct experimental evidence for the existence of such different R* conformations.

In conclusion, constitutive activation of mutated 5-HT_4Rs, classical family A GPCRs, can result from a change in the allosteric *J* constant, as we have shown previously (Claeysen *et al.*, 2000), and also to the formation of structurally distinct R*.

METHODS

Construction of truncated 5-$HT_{4(a)}$ receptor cDNA and epitope-tagged mutated and WT 5-$HT_{4(a)}$ receptors. Constructs were obtained as described (Claeysen *et al.*, 2000).

Construction of mutated m5-$HT_{4(a)}$ receptor cDNA: mutants A258L, D66N, C329S and C328–329S. Mutants were obtained by exchanging the endogenous amino acids in the m5-$HT_{4(a)}$R cDNA sequence, using the QuikChange™ Site-Directed Mutagenesis Kit (STRATAGENE).

Sense primer used for D66N: 5′-CTCGCCTTTGCT**AAC**CTGCTGGTT-3′

Sense primer used for C329S: 5′-ATCATCCTCTGC**AGT**GATGATGAGCG-3′

Sense primer used for C328–329S: 5′-ATCATCCTC**AGCAGT**GATGATGAGCGCTAC-3′.

Cell culture and transfection. The cDNA subcloned into pRK5, were introduced into COS-7 cells by electroporation, as described (Claeysen *et al.*, 2000).

Determination of cAMP production in intact cells. Six hours after transfection, cells were incubated overnight in DMEM without dialyzed fetal bovine serum (dFBS), but with 2 µCi [^{3}H]adenine/ml to label the ATP pool and cAMP accumulation was measured as described by (Dumuis *et al.*, 1988).

Membrane preparations and radioligand binding assay. Membranes were prepared from transiently transfected cells plated on 15 cm-dishes and grown in DMEM with 10% dFBS for 6 then 20 h in DMEM without dFBS as previously described (Ansanay *et al.*, 1996). Protein concentration in the samples was determined using the Bio-Rad protein assay (Bradford, 1976).

Binding studies on intact cells. To measure binding in intact cells, transiently transfected COS-7 cells were plated into 12-well clusters (5×10^5 cells/ml) and grown in DMEM with 10% dFBS for 6 and 20 h in DMEM without dFBS. Experiments were performed in HBS (20 mM HEPES, 150 mM NaCl, 4.2 mM KCl, 0.9 mM$CaCl_2$, 0.5 mM$MgCl_2$, 0.1% glucose, 0.1% BSA).The reaction mixture (250 µl) contained 0.4 to 0.6 nM [^{3}H]GR 113808 and 0.5 µM 5-HT was used to determine non-specific binding. Incubation lasted 2 h at 4°C and was terminated by rapid aspiration of the incubation buffer, followed by three washings in ice-cold HBS. Cells were then lysed in 0.1 N NaOH. Radioactivity was measured in 8 ml scintillation liquid PCS (Amersham).

Determination of receptor stability in membranes. Membranes (at 0.250 mg protein/ml) were incubated in binding buffer at 45 or 55°C. At $t = 0$ and after different periods of incubation, an aliquot (100 µl) was removed and used for a binding assay at a saturation concentration of [^{3}H]GR 113808 (0.4–0.6 nM), as described. We also made sure that the concentration of WT or mutated receptors was similar within a given experiment (see legends to figures).

Membrane preparations, gel electrophoresis and immunoblotting. Membranes were prepared from transiently transfected COS-7 cells expressing WT or mutated 5-HT$_4$ receptors as previously described (Claeysen *et al.*, 2000). The c-Myc antibodies were used at a dilution of 1:500 in the blocking buffer. The immunocomplexes were detected by enhancement using the chemiluminescence method (Renaissance Plus, NEN).

Immunocytochemical fluorescence labeling of epitope-tagged 5-HT$_4$Rs in cells. 5-HT$_4$Rs on intact cells were visualized using the anti-c-Myc primary antibody and a rhodamine conjugated secondary anti-mouse antibody. Cells were grown on coverslips and fixed 24 h after transient transfection in 4% paraformaldehyde diluted in PBS pH 7.4 for 30 min at room temperature, washed three times in a glycine buffer (0.1 M, pH 7.4) and incubated for 2 h at 37°C with the monoclonal antibody 9E10, ascitic fluid was diluted 1:250 in PBS-gelatin 0.2%. The cells were then washed and incubated for 1 h with a rhodamine-conjugated secondary anti-mouse antibody 1:40 in PBS-gelatin 0.2%. Coverslips were washed and mounted on glass slides using a gel mount (Biomeda Corp., Foster City, CA). Cells were viewed on a Bio-Rad CLSM 1024 confocal laser-scanning microscope. Rhodamine was exited at 568 nm.
All experiments have been done at least four times and data are expressed as the mean ± SEM.

Statistical analysis. We used least-square regressions to fit three models to the data: (α) linear without intercept $t_{1/2} = a\,(1 + J)$, (β) linear with intercept $t_{1/2} = a\,(1 + J) + b$, (γ) quadratic $t_{1/2} = a\,(1 + J)^2 + b(1 + J) + c$. The improvement of model fit between (α) and (β) and between (β) and (γ) provided a way for us to test the significance of the intercept and quadratic terms, respectively. The improvement between (α) and (β) was quantified as

$$F = \frac{(SS_{err,(\alpha)} - SS_{err,(\beta)})}{SS_{err,(\beta)}/df_{err,(\beta)}}$$

, where $SS_{err,(\alpha)}$ and $SS_{err,(\beta)}$ are, respectively, the error sums of squares of models (α) and (β) and df is the degree of freedom. The significance was assessed by comparing F to an F-

distribution with 1 and $df_{err,(\beta)}$ degrees of freedom. A similar procedure was used to compare models (β) and (γ).

ACKNOWLEDGEMENTS

We are grateful to J.-P. Pin, O. Manzoni, and L. Fagni for valuable discussions and to P. David for the statistical analysis. A.L. Turner-Madeuf and F. Carroll are acknowledged for their help in the writing of the manuscript and M. Passama for preparation of figures.

REFERENCES

Alewijnse A.E., Timmerman, H., Jacobs, E.H., Smit, M.J., Roovers, E., Cotecchia, S. and Leurs, R. (2000) The effect of mutations in the DRY motif on the constitutive activity and structural instability of the histamine H(2) receptor. Mol. Pharmacol., 57, 890–898.

Ansanay H., Sebben, M., Bockaert, J. and Dumuis, A. (1996) Pharmacological comparison between [^{3}H]-GR113808 binding sites and 5-HT$_4$ receptors coupled to adenylyl cyclase in mouse colliculi neurons. Eur. J. Pharmacol. (Mol. Pharmacol. Section), 298, 165–174.

Bockaert J. and Pin, J.P. (1999) Molecular tinkering of G protein-coupled receptors: an evolutionary success. EMBO J., 18, 1723–1729.

Bradford M.M. (1976) A rapid and sensitive method for the quantitation of microgram quantities of protein utilising the principle of protein-dye binding. Anal. Biochem., 72, 248–254.

Claeysen S., Sebben, M., Bécamel, C., Eglen, R., Clark, R.D., Bockaert, J. and Dumuis, A. (2000) Pharmacological properties of the 5-hydroxytryptamine$_4$ receptor antagonists on constitutively active wild-type and mutated receptors. Mol. Pharmacol., 58, 136–144.

Dumuis A., Sebben, M. and Bockaert, J. (1988) Pharmacology of 5-hydroxytryptamine$_{1A}$ receptors which inhibit cAMP production in hippocampal and cortical neurons in primary culture. Mol. Pharmacol., 33, 178–186.

Fanelli F., Barbier, P., Zanchetta, D., de Benedetti, P.G. and Chini, B. (1999) Activation mechanism of human oxytocin receptor: a combined study of experimental and computer-simulated mutagenesis. Mol. Pharmacol., 56, 214–225.

Gether U., Ballesteros, J.A., Seifert, R., Sanders-Bush, E., Weinstein, H. and Kobilka, B.K. (1997) Structural instability of a constitutively active G protein-coupled receptor. Agonist-independent activation due to conformational flexibility. J. Biol. Chem., 272, 2587–2590.

Gether U. and Kobilka, B.K. (1998) G protein-coupled receptors. II. Mechanism of agonist activation. J. Biol. Chem., 273, 17979–17982

Gudermann T., Kalkbrenner, F. and Schultz, G. (1996) Diversity and selectivity of receptor-G protein interaction. Ann. Rev. Pharmacol. Toxicol., 36, 429–459.

Kenakin T. (1995) Agonist-receptor efficacy I: mechanisms of efficacy and receptor promiscuity. Trends Pharmacol. Sci., 16, 188–192.

Kenakin T. (1996) The classification of seven transmembrane receptors in recombinant expression systems. Pharmacol. Rev., 48, 413–463.

Kenakin T. (1997) Agonist-specific conformations. Trends Pharmacol. Sci., 18, 416–417.

Kjelsberg M.A., Cotecchia, S., Ostrowski, J., Caron, M.C. and Lefkowitz, R.J. (1992) Constitutive activation of the α_{1B}-adrenergic receptor by all amino acid substitutions at a single site. J. Biol. Chem., 267, 1430–1433.

Leff P. (1995) The two-state model of receptor activation. Trends Pharmacol., 16, 89–97.

Moffett S., Adam, L., Bonin, H., Loisel, T.P., Bouvier, M. and Mouillac, B. (1996) Palmitoylated cysteine 341 modulates phosphorylation of the β2-adrenergic receptor by the cAMP-dependent protein kinase. J. Biol. Chem., 271, 21490–21497.

Monod J., Wyman, J. and Changeux, J.-P. (1965) On the nature of allosteric transitions: a plausible model. J. Mol. Biol., 12, 88–118.

Onaran H.O. and Costa, T. (1997) Agonist efficacy and allosteric models of receptor action. Ann. N. Y. Acad. Sci., 812, 98–115.

Palczewski K., *et al.* (2000) Crystal structure of rhodopsin: A G protein-coupled receptor. Science, 289, 739–745.

Parma J., Van Sande, J., Swillens, S., Tonacchera, M., Dumont, J. and Vassart, G. (1995) Somatic mutations causing constitutive activity of the thyrotropin receptor are the major cause of hyperfunctioning thyroid adenomas: identification of additional mutations activating both the cyclic adenosine 3′,5′-monophosphate and inositol phosphate-Ca^{2+} cascades. Mol. Endocrinol., 9, 725–733.

Samama P., Cotecchia, S., Costa, T. and Lefkowitz, R.J. (1993) A mutation-induced activated state of the β_2-adrenergic receptor. Extending the ternary complex model. J. Biol. Chem., 268, 4625–4635.

Scheer A., Fanelli, F., Costa, T., De Benedetti, P.G. and Cotecchia, S. (1996) Constitutively active mutants of the α_{1B}-adrenergic receptor: role of highly conserved polar amino acids in receptor activation. EMBO J., 15, 3566–3578.

Sealfon S.C., Chi, L., Ebersole, B.J., Rodic, V., Zhang, D., Ballesteros, J.A. and Weinstein, H. (1995) Related contribution of specific helix 2 and 7 residues to conformational activation of the serotonin 5-HT_{2A} receptor. J. Biol. Chem., 270, 16683–16688.

Spengler D., Waeber, C., Pantaloni, C., Holsboer, F., Bockaert, J., Seeburg, P.H. and Journot, L. (1993) Differential signal transduction by five splice variants of the PACAP receptor. Nature, 365, 170–175.

Spiegel A.M. (1996) Defects in G protein-coupled signal transduction in human disease. Annu. Rev. Physiol., 58, 143–170.

Tiberi M. and Caron, M.G. (1994) High agonist-independent activity is a distinguishing feature of the dopamine D1B receptor subtype. J. Biol. Chem., 269, 27925–27931.

Van Sande J., Parma, J., Tonacchera, M., Swillens, S., Dumont, J. and Vassart, G. (1995) Somatic and germline mutations of the TSH receptor gene in thyroid diseases. J. Clin. Endocrinol. Metab., 80, 2577–2585.

Wang C.D., Buck, M.A. and Fraser, C.M. (1991) Site-directed mutagenesis of α2A-adrenergic receptors: identification of amino acids involved in ligand binding and receptor activation by agonists. Mol. Pharmacol., 40, 168–179.

FIGURE LEGENDS

Figure 1. Constitutively active mutated 5-HT_4 receptors showed thermal instability compared with WT receptors. WT, 5-HT_4R (Δ327) and 5-HT_4R (A258L) mutant (Claeysen *et al.*, 2000) receptors were transiently expressed in COS-7 cells at 2800 ± 340, 2560 ± 180 and 2900 ± 320 fmol/mg protein, respectively. (**A**) Basal and 5-HT-stimulated activation of WT, 5-HT_4R (Δ327) and 5-HT_4R (A258L) were evaluated by measuring the accumulation of cAMP over a period of 20 min. The percentage conversion of [^{3}H]ATP to [^{3}H]cAMP in mock was 0.12 ± 0.04. (**B**) Membranes were incubated at 45 or 55°C for 3 h. Data are given as remaining [^{3}H]GR 113808 binding as a percentage of maximum specific binding at t = 0. (**C**) Membranes expressing receptors were incubated at 55°C for indicated periods of time. The remaining [^{3}H]GR 113808 binding (B) is given as a percentage of maximum binding at t = 0 (Rt0). (**D**) Semi-logarithmic plot of the curve showing the evolution of the Rt/Rt0 ratio as a function of time. (**E**) Western blot analysis of c-myc epitope tagged WT and Δ327 5-HT_4R before and after incubation at 55°C for 180 min. The WT receptor is shown at a 42 kDa band, the Δ327 receptor at a 34 kDA band. The non-specific labeled band at 45 kDa indicates that nearly the same amount of proteins has been applied on the gel.

Figure 2. Comparison between cellular distribution of mutated A258L and Δ327 and WT 5-HT_4 receptors. (**A**) cDNA (300 and 150 µg) coding for epitope-tagged mutated and WT 5-$HT_{4(a)}$ receptors respectively, were transiently transfected in COS-7 cells to obtain nearly similar expression receptor levels. Confocal microscopic images show that rhodamine-conjugated secondary anti-mouse antibody fluorescence was predominantly confined to the plasma membranes. These images are representative of four independent experiments. (**B**) cDNA coding for WT, A258L and Δ327 receptors [same concentration as in (A)], were transiently transfected in COS-7 cells. Receptor density was measured both in COS-7 cells, in membranes and on intact cells using [^{3}H] GR 113808 at saturating concentrations. A/B is the ratio between the number of [^{3}H] GR 113808 binding sites/cell determined in intact cells and particulate fractions.

Figure 3. Thermal instability of a series of 5-HT_4R mutants: evidence for the existence of different R* conformations. (**A**) Schematic representation of the mutated 5-$HT_{4(a)}$ receptors used in this study. (**B**) Basal and 5-HT-stimulated cAMP formation in COS-7 cells expressing WT and different truncated and mutated 5-HT_4Rs in C-terminal tail and in the i3 loop (WT,

Δ358, Δ346, Δ327, C329S and C328–329S, A258L). (**C**) WT, Δ358, Δ346, Δ327, C329S, C328–329S, A258L receptors were transiently expressed in COS-7 cells at 1750 ± 140, 1980 ± 180, 1670 ± 120, 2070 ± 210, 1980 ± 120, 2130 ± 160 fmol/mg protein, respectively. cAMP formation was evaluated by measuring the accumulation of cAMP over a period of 20 min and expressed as a percentage of mock transfected cells. The percentage conversion of [^{3}H]ATP to [^{3}H]cAMP in mock transfected COS-7 cells was 0.15 ± 0.03. (**D**) Relationship between the $t_{1/2}$ of denaturation of WT and mutated 5-HT$_4$ receptors and the allosteric *J* constant. The $t_{1/2}$ of the WT and different mutants were determined as in Figure 1. The *J* constants of WT, Δ327, A258L receptors have been determined previously (Claeysen *et al.*, 2000) and were equal to 6.12 ± 0.48, 1.22 ± 0.25 and 0.78 ± 0.05, respectively. Those of Δ358, Δ346, C328–329S, C329S were calculated as described previously (Claeysen *et al.*, 2000) and were equal to 5.95 ± 0.35, 2.18 ± 0.26, 2.36 ± 0.24, 3.64 ± 0.18, respectively. The regression $t_{1/2} = a\ (1 + J)$ is positive and significant when A258L is excluded (a = 9.7 ± SE 0.46, $p < 0.0001$).

Fig. 4. Mutation of the conserved Asp residue in TMDII of GPCRs (family 1) leads to a particularly silent receptor, structurally more stable than the WT receptor. (**A**) WT and D66N basal activities were plotted as a function of receptor expression levels. WT and D66N receptors were transiently expressed at variable levels by transfecting increasing amounts of specific plasmid. Basal activities were evaluated by measuring the accumulation of cAMP over a period of 20 min and expressed as a percentage of mock transfected cells. The percentage conversion of [^{3}H]ATP to [^{3}H]cAMP in mock transfected COS-7 cells was 0.18 ± 0.03. (**B**) Semi-logarithmic representation of the curve showing the evolution of the Rt/Rt0 ratio as a function of incubation time at 55°C.

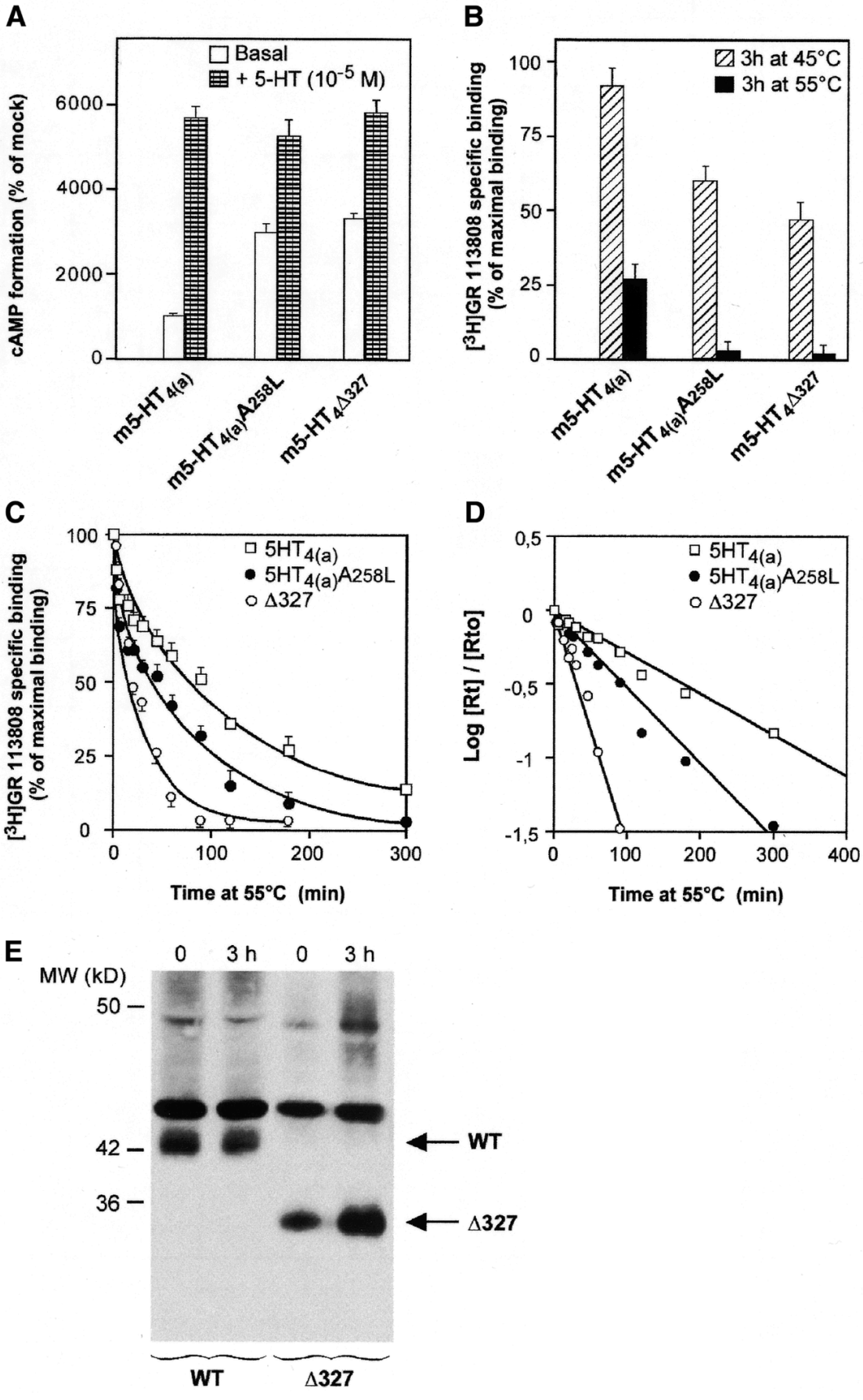
A
Basal
+ 5-HT (10-5 M)
cAMP formation (% of mock)
6000
4000
2000
0
m5-HT4(a)
m5-HT4(a)A258L
m5-HT4Δ327
B
3h at 45°C
3h at 55°C
[3H]GR 113808 specific binding (% of maximal binding)
100
75
50
25
0
m5-HT4(a)
m5-HT4(a)A258L
m5-HT4Δ327
C
5HT4(a)
5HT4(a)A258L
Δ327
[3H]GR 113808 specific binding (% of maximal binding)
100
75
50
25
0
0
100
200
300
Time at 55°C (min)
D
5HT4(a)
5HT4(a)A258L
Δ327
Log [Rt] / [Rto]
0,5
0
-0,5
-1
-1,5
0
100
200
300
400
Time at 55°C (min)
E
0
3 h
0
3 h
MW (kD)
50
42
36
WT
Δ327
WT
Δ327

Figure 1

A

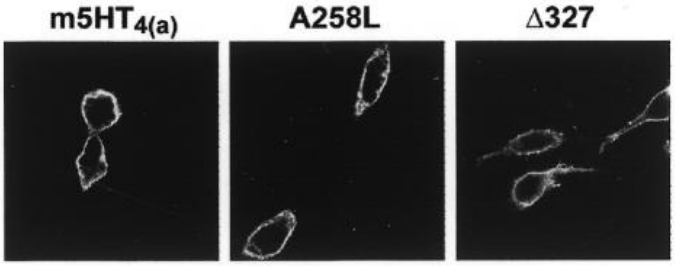

B

Receptors	A Number of sites / cell	B fmol/mg protein in cell membranes	A / B
5-HT$_{4(a)}$	$2.18 \times 10^5 \pm 0.15$	2800 ± 340	77.85
A258L	$1.92 \times 10^5 \pm 0.21$	2560 ± 180	75
Δ327	$2.27 \times 10^5 \pm 0.07$	2900 ± 320	78.27

Figure 2

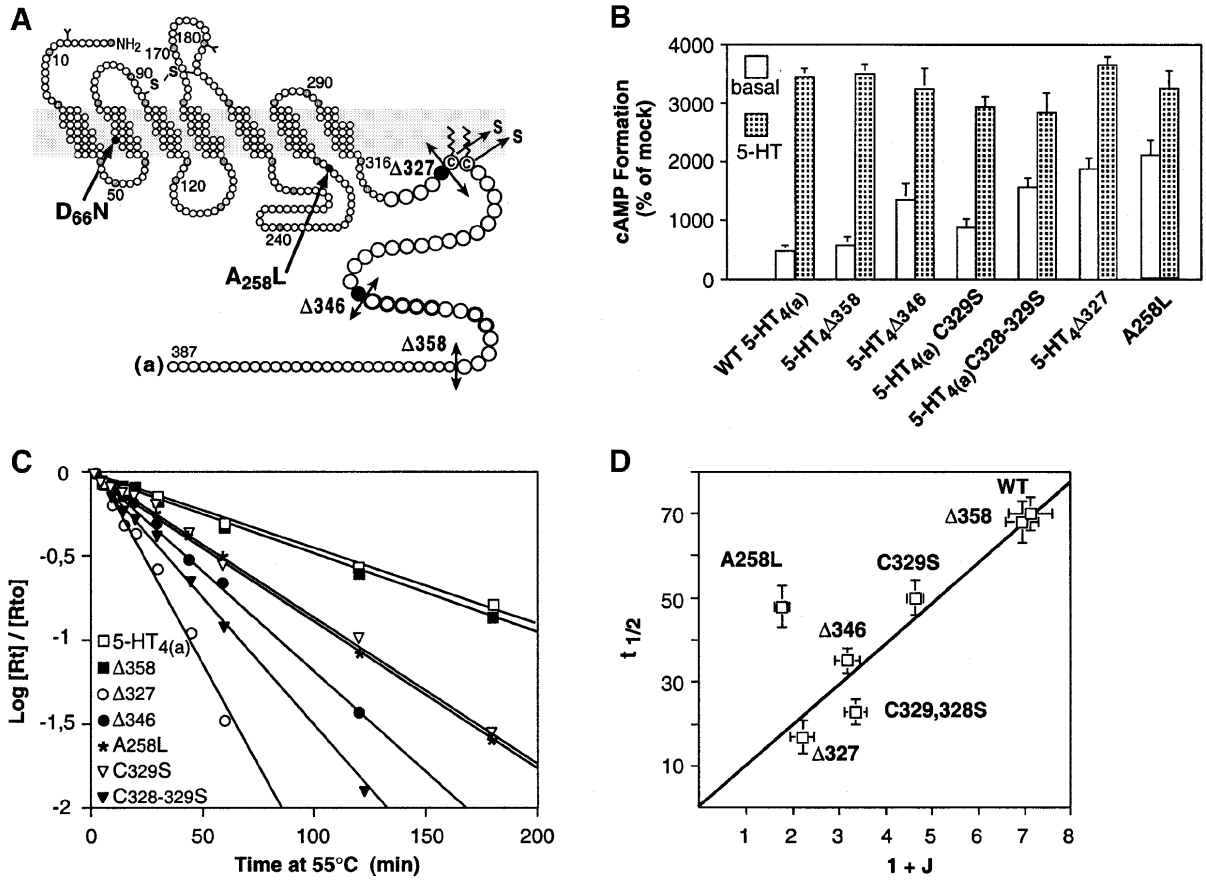
A
NH2
10
170
180
90
290
316
Δ327
120
50
D66N
240
A258L
Δ346
Δ358
387
(a)
B
cAMP Formation (% of mock)
4000
3000
2000
1000
0
basal
5-HT
WT 5-HT4(a)
5-HT4Δ358
5-HT4Δ346
5-HT4(a) C329S
5-HT4(a)C328-329S
5-HT4Δ327
A258L
C
Log [Rt] / [Rto]
0
-0,5
-1
-1,5
-2
5-HT4(a)
Δ358
Δ327
Δ346
A258L
C329S
C328-329S
0
50
100
150
200
Time at 55°C (min)
D
t 1/2
70
50
30
10
WT
Δ358
A258L
C329S
Δ346
C329,328S
Δ327
1
2
3
4
5
6
7
8
1 + J

Figure 3

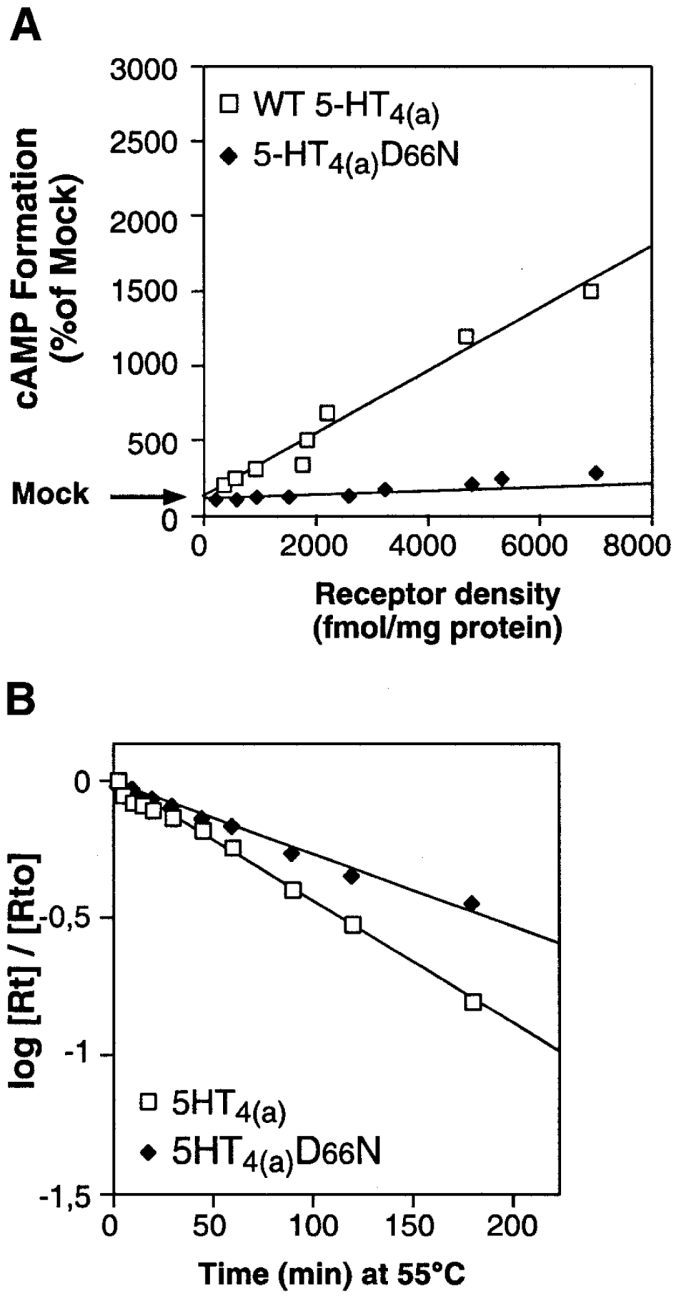
A
cAMP Formation (%of Mock)
3000
2500
2000
1500
1000
500
Mock
0
WT 5-HT4(a)
5-HT4(a)D66N
0
2000
4000
6000
8000
Receptor density (fmol/mg protein)
B
log [Rt] / [Rto]
0
-0,5
-1
-1,5
5HT4(a)
5HT4(a)D66N
0
50
100
150
200
Time (min) at 55°C

Figure 4